

Sol-gel synthesis and properties of Sm modified TiO₂ nanopowders

S. I. Yordanov¹, A. D. Bachvarova-Nedelcheva^{2*},
R. S. Iordanova², I. D. Stambolova²

¹ Institute of Metal Science, equipment, and technologies “Acad. A. Balevski”
with Center for Hydro- and Aerodynamics at the Bulgarian Academy of Sciences,
67 Shipchenski prohod str., 1574 Sofia, Bulgaria

² Institute of General and Inorganic Chemistry, Bulgarian Academy of Sciences,
Acad. G. Bonchev str., bld. 11, 1113 Sofia, Bulgaria

Received November 11, 2018; Accepted November 28, 2018

The present investigation deals with the sol-gel synthesis and properties of samarium doped TiO₂ nanopowders and the impact of Sm³⁺ on the structural and thermal properties of the obtained samples was established. By XRD was found that the heat treated up to 300 °C gels exhibit a predominantly amorphous phase and its amount gradually decreases with increasing the temperature (above 400 °C). The first TiO₂ (anatase) crystals were detected at about 400 °C and the average crystallite size of the samples heat treated at 400 °C is about 25–30 nm. By DTA was established that the organics decomposition is accompanied by strong weight loss occurring in the temperature range 240–350 °C. The completeness of the hydrolysis – condensation reactions was verified by IR and UV-Vis analyses.

Keywords: sol-gel, powders, thermal stability, X-ray diffraction.

INTRODUCTION

It is well known that TiO₂, especially its anatase phase, has been recognized as the preferable one for photocatalytic degradation of organic pollutants and other environmental applications due to its high photosensitivity, strong oxidizing power, nontoxic nature, and chemical stability [1–3]. Titanium dioxide is also a promising wide-gap (3.2 eV) semiconductor which appears to be suitable host for the introducing of different ions such as noble metals, transition metals, lanthanide cations, as well as anions of non-metal elements, which usually could be introduced by oxides, salts, sulfides, halogenides or more complex compounds [1–5]. Among the different dopants, the rare earth (RE) impurities have been recognized as most effective to achieve efficient emission in the visible range [1, 2]. Recently, lanthanides have been widely investigated due to their electronic, optical and chemical characteristics arising from their 4f electrons. It has been shown that the doping only with a few rare earth ions (Nd³⁺,

Eu³⁺, La³⁺, Er³⁺ and Sm³⁺) lead to a significant impact on the TiO₂ properties [6–12]. To best of our knowledge, the synthesis, characterization and optical properties of sol-gel derived Sm doped TiO₂ have not been studied in details. Up to now, for the preparation of Sm doped TiO₂ composites, mainly two methods (sol-gel and hydrothermal) have been applied [13–16]. It is proved that the sol-gel method is an excellent technique to prepare both oxides thin films and powders and it allows syntheses in a wide range of compositions using a variety of precursors. On the other hand, by sol-gel technique can be obtained materials with high TiO₂ content which usually need high temperatures for synthesis. Powders can be easily characterized applying different techniques but not all of them are applicable to films. The information obtained for the powders could be helpful to determine the experimental conditions for the sol-gel synthesis of the films as well as for the prediction of their thermal behavior and properties.

Our team has gained experience in the study of sol-gel synthesis, characterization and properties of pure and modified nanosized TiO₂ powders [17–21]. In our previous papers, many problems regarding the influence of precursors during the synthesis, phase formation upon heating of the gels, thermal stability and properties of the ob-

* To whom all correspondence should be sent:
E-mail: albenadb@svr.igic.bas.bg

tained powdered products were studied but there are still unclarified points. The present study continues our investigations for obtaining of pure and modified TiO₂ nanopowders applying the sol-gel technique.

The rare earth doped TiO₂ thin films obtained by sol-gel method exhibited good anticorrosion properties [22, 23]. Our investigations on Sm doped TiO₂ films are still in course and they showed increased corrosion resistance. Due to the existing restrictions for structural characterization of the films and in order to achieve better understanding of the relationship “composition – structure – property – application”, powders with the same Sm/TiO₂ compositions have been prepared. In the present work the attention is paid to the phase and structural characterization as well as thermal properties of sol-gel derived Sm modified TiO₂ nanopowders.

EXPERIMENTAL

Samples preparation

Ti(IV) butoxide (TBT, Merck), Samarium oxide (Sm₂O₃) (Janssen Chimica, Belgium 99,9%), isopropanol (i-PrOH, >99.5%, Merck) have been used as main precursors for the obtaining of titania powders. The acetylacetonate (acac, Sigma-Aldrich) was used as a chelating agent to form stable complexes with TBT. The experimental conditions for obtaining the initial solutions for powders and films are identical and they consisted of several steps. The first solution was prepared by mixing of TBT, i-PrOH and AcAc at vigorous stirring while keeping the molar ratio TBT/C₃H₇OH/AcAc = 1:30:1. The resulting solution was transparent with orange color which is typical for the formed chelate complex. The other solution was obtained by Sm₂O₃ dissolved in 1.5 ml HNO₃ and isopropanol. Finally, both solutions were mixed at vigorous stirring. During the experimental procedure no additional water was added. The sol-gel hydrolysis reaction was accomplished only in presence of air moisture. The pH of as-prepared solutions was measured to be between 4 and 5. The ageing of the gels was performed in air for several days in order to allow further hydrolysis. Aiming to verify the phase transformations, all gels were subjected to stepwise heating in air from 200 to 700 °C for one hour exposure time for each temperature. The heat treatment regime has been selected on the basis of our previous investigations. Three different samarium concentrations have been selected for modification of TiO₂ in the synthesized samples – 0.5, 1 and 2 mol%. The investigated samples were denoted as follow: TBT/0.5%Sm, TBT/1%Sm and TBT/2%Sm.

Samples characterization

XRD patterns on powdered samples were registered at room temperature with a Bruker D8 Advance diffractometer using CuK_α radiation. The thermal behavior of the gels dried at room temperature was determined by differential thermal analysis (LABSYSTM EVO apparatus) with Pt-Pt/Rh thermocouple at a heating rate of 10 K/min in air flow, using Al₂O₃ as a reference material. The accuracy of the temperature maintenance was determined as ±5 °C. Gases evolved (EGA) during the thermal treatments were analyzed by mass spectrometry (MS) with a Pfeiffer OmniStar™ mass spectrometer. Mass spectra recorded for samples show the m/z = 14, 15, 18 and 44 signals, being ascribed to CH₂, CH₃, H₂O and CO₂, respectively. The IR spectra were registered in the range 1600–400 cm⁻¹ using the KBr pellet technique on a Nicolet-320 FTIR spectrometer with 64 scans and a resolution of ±1 cm⁻¹. The specific surface area of samples heat treated at 500 °C was measured using BET analysis (Quantachrome Instruments NOVA 1200e (USA) apparatus). The optical absorption spectra of the powdered samples in the wavelength range 200–800 nm were recorded at room temperature using a UV-Vis diffused reflectance spectrophotometer “Evolution 300” using a magnesium oxide reflectance standard as the baseline fort wavelengths in the range of 200–1000 nm. The absorption edge and the optical band gap were determined following Dharma et al. instructions [24]. The band gap energies (E_g) of the samples were calculated by the Planck’s equation: $E_g = hc/\lambda$, where E_g is the band gap energy (eV), h is the Planck’s constant (eV s), c is the light velocity (m/s), and λ is the wavelength (nm).

RESULTS AND DISCUSSION

Phase transformations and thermal stability

All prepared gels were transparent with bright orange color. The XRD patterns of gels and heat treated samples in the temperature range 200–700 °C are shown in Fig. 1. The analysis of the results showed that the X-ray diffraction patterns of sample TBT/1%Sm are identical to those of sample TBT/2%Sm and only the latter were presented. Samarium phases were not registered by X-ray diffraction analysis. As it is seen in both samples (TBT/0.5%Sm and TBT/2%Sm) the amorphous phase is dominant up to 300 °C. The first crystals of TiO₂ (anatase) (ICDD 78-2486) are registered at 400 °C which is the main crystalline phase up to 700 °C. From Fig. 1 it could be seen that the increasing of calcination temperature led to an in-

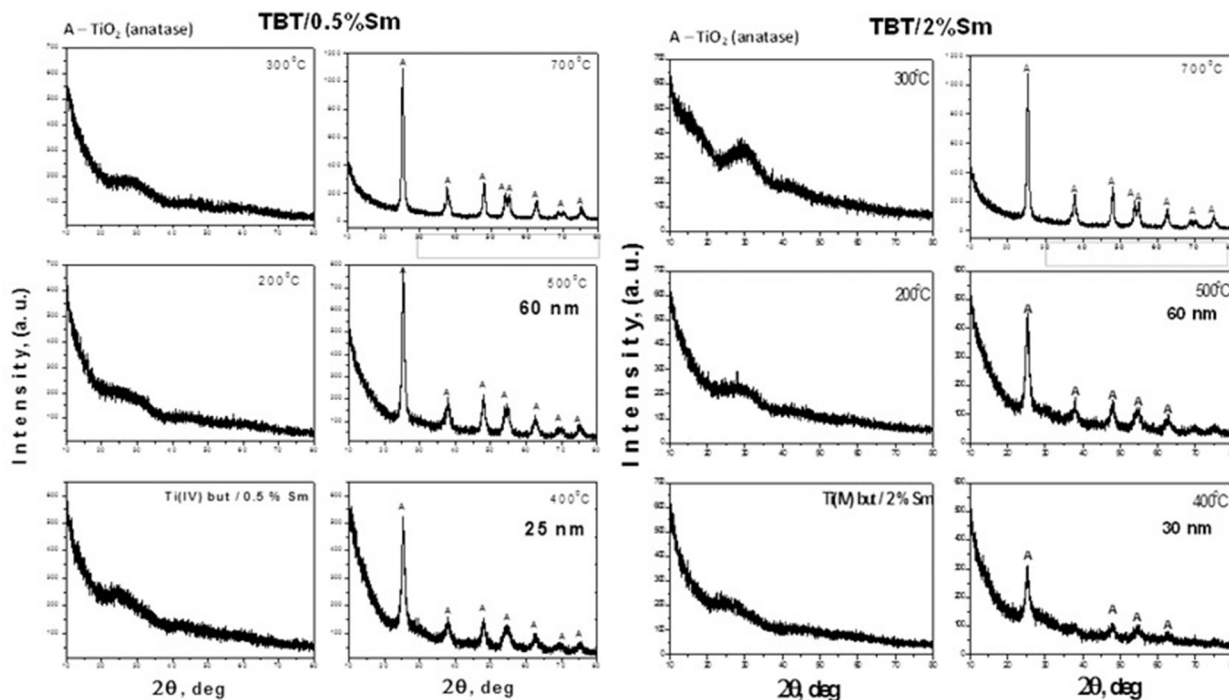


Fig. 1. XRD patterns of the investigated compositions Ti/0.5%Sm and Ti/2%Sm heat treated in the temperature range 200–700 °C.

crease of the peak intensity of anatase. The main diffraction peak becomes narrow which indicated enhanced crystallinity. At 400 °C the average crystallite size (calculated using Sherrer's equation) of TiO₂ (anatase) in all samples is about 25–30 nm (Fig. 1). At higher temperature (500 °C) faster crystal growth occurs which is proved by the increased particles size (60 nm). The preliminary investigations on the phase formation of the sol-gel derived Sm doped TiO₂ thin films with the same composition did not show any differences in comparison with the as-prepared powders.

Our results concerning the influence of calcination temperature on the phase formation of investigated samples are in good agreement with those obtained in the literature [13, 25, 26]. It is worth noting that the phase transition TiO₂ (anatase) → TiO₂ (rutile) was not registered even at 700 °C and it could be suggested that the presence of samarium hindered the crystallization of TiO₂ (rutile). The specific surface areas (SBET) of samples TBT/0.5%Sm and TBT/2%Sm were measured and they are 21 and 81 m²/g, respectively. For comparison, the specific surface area of pure Ti(IV) n-butoxide is 21 m²/g. This higher value of the specific surface area for the sample TBT/2%Sm could predict potential good environmental applications.

The thermal stability of gels aged at room temperature was investigated by simultaneous thermo-

gravimetric (TG) and differential thermal analysis (DTA). The DTA/TG curves are presented for both gels – TBT/0.5%Sm (Fig. 2a,b), TBT/2%Sm (Fig. 2c, d) and several stages could be marked on them. Probably, the higher amount of organic groups due to presence of solvent and chelating agent led to the stepwise release of the organics. The common feature is the presence of a weak endothermic effect near 75–80 °C which is the first decomposition step of the gels (Fig. 2a–d). This step could be assigned to the evaporation of physically adsorbed water and/or organic solvent (isopropanol). The average mass loss after dehydration is about 10% for sample TBT/0.5%Sm (Fig. 2a, b) and ~15% for the other sample TBT/2%Sm (Fig. 2c, d). The first exothermic peaks in the TBT/0.5%Sm and TBT/2%Sm samples are at about 280 and 245 °C, respectively (Fig. 2a–d) and they both are accompanied by the mass loss of ~10% that could be related to the combustion of alkoxide groups bonded to Ti-atom. Obviously, at lower samarium concentration, the exothermic effect is shifted to higher temperature (280 °C) in comparison to the other sample containing higher amount of Sm for which the exothermic peak is positioned at 245 °C. The next stronger exothermic effects are at about 340 and 345 °C. Bearing in mind that the mass loss of this stage is ~10%, it could be assigned both to the combustion of residual organic groups as well as probably the beginning of

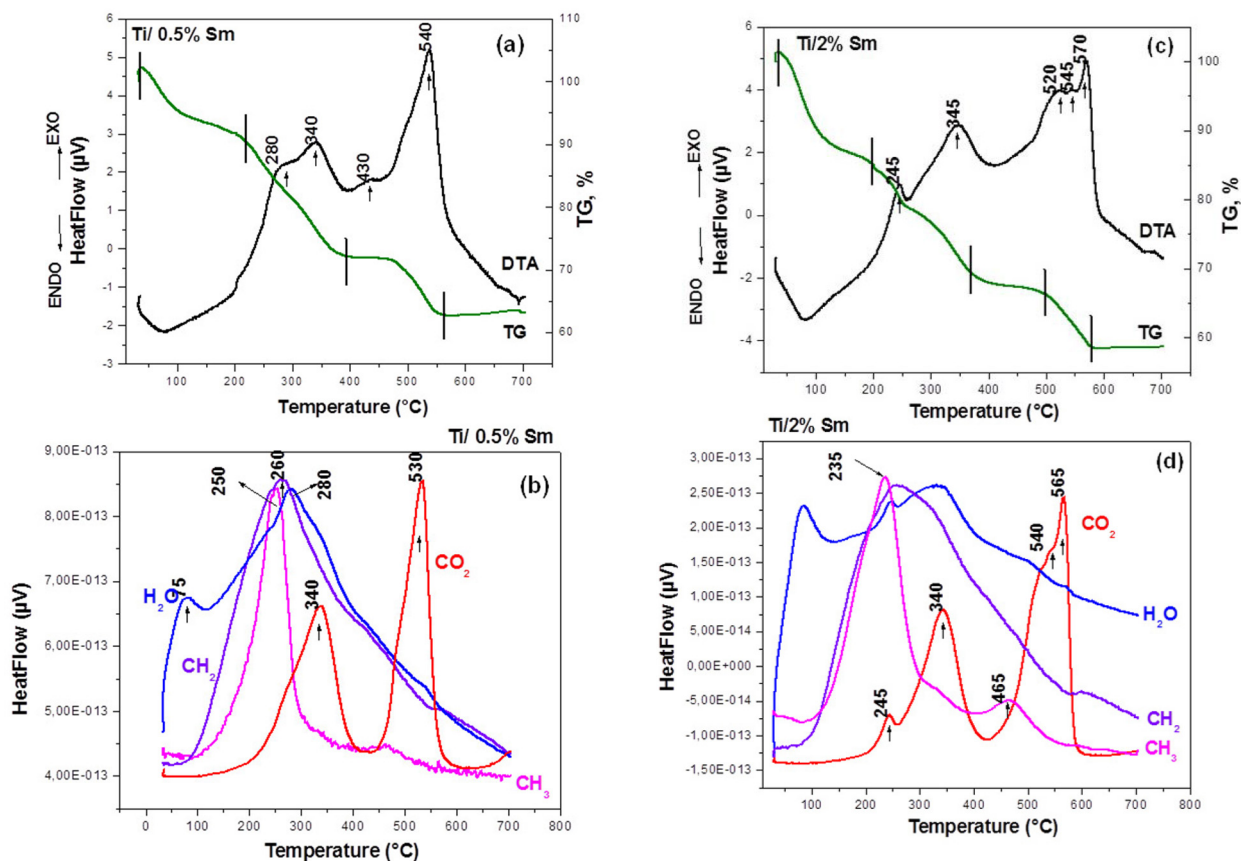


Fig. 2. *a–b*, DTA/TG curves of the Ti/0.5% Sm; *c–d*, DTA/TG curves of the Ti/2% Sm.

the TiO₂ (anatase) crystallization. As it is seen there is a difference in the thermal behavior of the investigated samples above 500 °C. The comparison of the DTA-TG curves of the samples showed that one exothermic effect at about 540 °C is observed in the TBT/0.5%Sm gel while in the other one, three consecutive exothermic effects were detected (at 520 °C, 545 °C and 570 °C). It is also obvious that in both cases a mass loss of about 10 % is observed. On the basis of these experimental facts it could be assumed that the effects in the range 520–540 °C could be related to the oxidation of residual carbon and release of CO₂. The last exothermic effects at 570 °C observed only in the sample TBT/2%Sm is very strong and it could be associated to the intensive crystallization of anatase (Fig. 2c, d). The results obtained by DTA correspond well to the above pointed XRD data (Fig. 1) as well as to the results obtained by other authors for Sm doped powders [27].

IR and UV-Vis characterization

The IR spectroscopy was used mainly to evaluate the rate and degree of hydrolysis and condensa-

tion processes in the prepared gels and heat treated samples. The IR spectra of investigated samples are presented in Fig. 3. The vibrational spectra of pure Ti(IV) butoxide as well as of 2-propanol were shown and discussed already elsewhere [28–31]. By analogy with our previous papers, the assignments of the vibrational bands of separate structural units are made on the basis of well-known spectral data for Ti(IV) *n*-butoxide, isopropanol and crystalline TiO₂ (anatase). Looking at Figure 3, intensive bands are observed in the IR spectra of the gels and their intensities decreased with the increasing of temperature. No differences could be seen regarding the position and intensity of the bands for the heat treated samples (TBT/0.5%Sm and TBT/2%Sm) in the range 200–500 °C. Generally, the bands located between 1500–1300 cm⁻¹ are assigned to the bending vibrations of CH₃ and CH₂ groups. The band at 1120 cm⁻¹ is characteristic for the stretching vibrations of Ti-O-C, while those at 1190 and 1020 cm⁻¹ are assigned to the vibrations of terminal and bridging C-O bonds in butoxy ligands [28, 32–34]. The absorption bands below 1000 cm⁻¹ in the samples correspond to C-H, C-O and deformation Ti-O-C vibrations [32, 35]. In our previous inves-

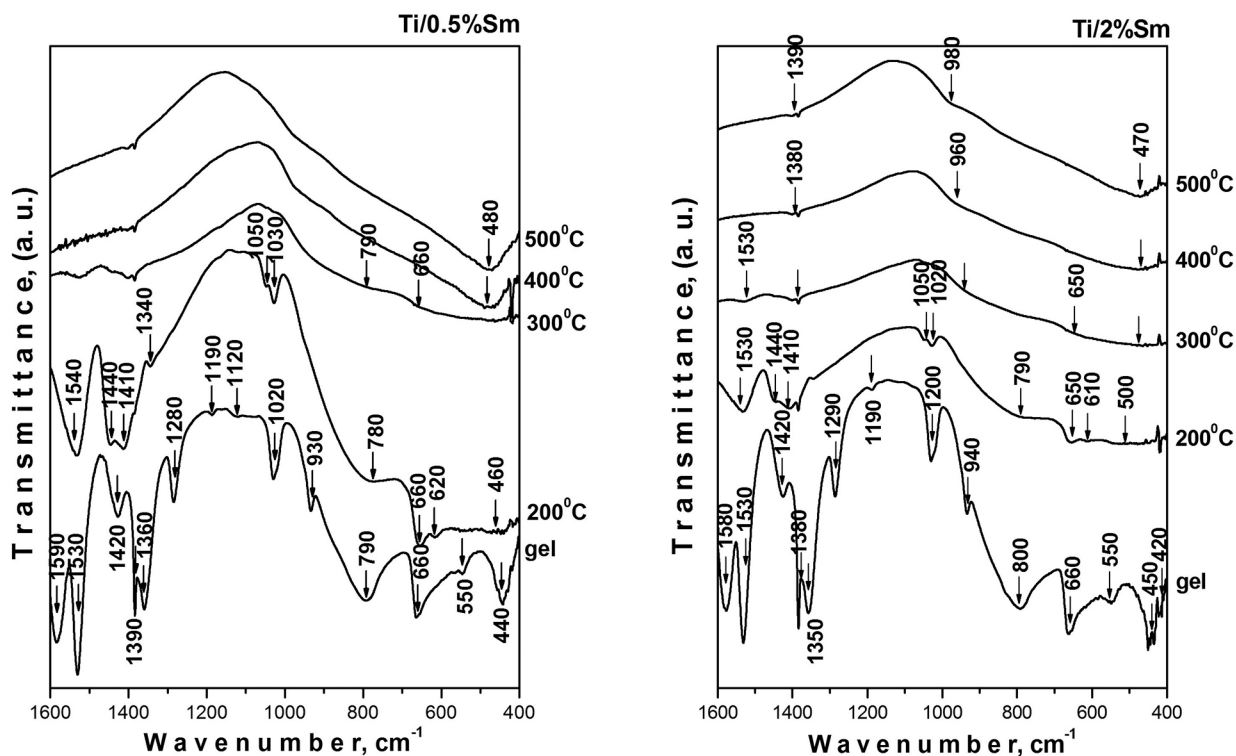


Fig. 3. IR spectra of Ti/0.5%Sm, Ti/1% Sm and Ti/2%Sm gels and heat treated up to 500 °C samples.

tigations [30, 31] it was found that the absorption region 1100–1020 cm⁻¹ is very complex due to the overlapping of the vibrations of different structural units from the alkoxide and solvent. In spite of that, many authors [36–38] use these bands for the interpretation of the degree of hydrolysis-condensation processes. The bands below 800 cm⁻¹ correspond to the vibrations of TiO₆ units [36, 37]. Bearing in mind that the typical Sm – O stretching vibrations are in the range 510–430 cm⁻¹ [39] an overlapping between the inorganic structural polyhedral is suggested. The obtained by us IR spectra of pure Ti(IV) butoxide [29–31] and Sm/TiO₂ were compared and it was established that the Sm doping did not influence the short range order of the resulting products.

The UV-Vis spectroscopy is used in order to obtain additional structural information for the investigated samples as well as to evaluate the completeness of hydrolysis – condensation processes. The spectra of gels (25 °C) {Ti(IV) n-butoxide, TBT/0.5%Sm and TBT/2%Sm} are presented in Fig. 4. The interpretation of the UV-Vis spectra is made on the basis of literature data as well as our previous results obtained in various systems containing TiO₂ [30, 31, 36, 37, 40–42]. Looking at the UV-Vis spectra of investigated samples several peaks could be distinguished. Bands at 250 and

320 nm are observed in the spectrum of pure Ti(IV) n-butoxide gel, while those at 260, 340–350 and 360 nm were detected for the samarium doped TiO₂ gels. A red shift of the absorption edge in the Sm doped TiO₂ powders (431.98 nm – TBT/0.5%Sm

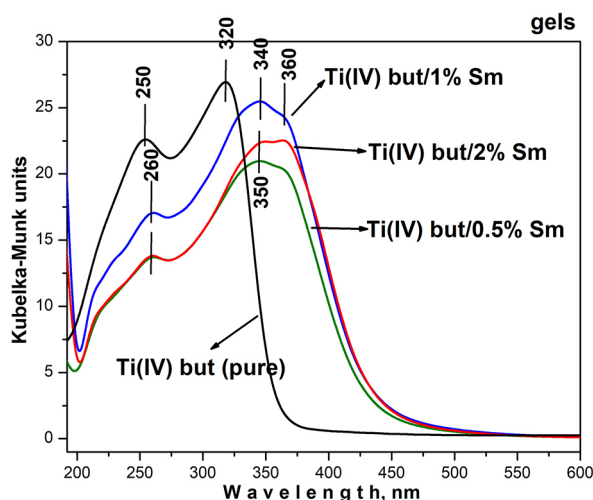


Fig. 4. UV-Vis spectra of Ti/0.5%Sm, Ti/1% Sm and Ti/2%Sm gels and heated at 200 °C samples.

Table 1. Observed cut-off and calculated optical band gap values (E_g) of the obtained gels

Compositions, mol%	UV-Vis results	
	E _g , eV	cut-off, nm
TiO ₂ (Ti(IV) n-butoxide)	3.8	389.71
(Ti(IV) butoxide/0.5% Sm	2.9	431.98
(Ti(IV) butoxide/2% Sm	2.8	439.26

and 439.26 nm – TBT/2%Sm) are clearly observed in comparison to pure TiO₂ gel (389.71 nm). The higher cut-off value (439.26 nm) of sample TBT/2%Sm is due to the increased absorption in the Vis region as a result of the higher concentration of samarium. The calculated values of band gap energy (E_g) of pure TBT and samarium doped gels (aged at room temperature) are 3.8, 2.9 and 2.8 eV, respectively (Table 1). By analogy with our previous investigations [29–31] the two maxima about 250–260 nm and 320–350 nm could be related to the isolated TiO₄ and polymerized TiO₆ groups, respectively. As it was already shown elsewhere [29, 30, 37], during the hydrolysis – condensation processes the coordination geometry is changed from TiO₄ to TiO₆ as a result of polymerized Ti species (Ti–O–Ti links between TiO₆ units) [37]. The higher ratio between the bands intensity at 260 and 340 nm (350 nm) for sample TBT/1%Sm as compared to the other samples, is clear indication for the greater degree of hydrolysis and condensation processes in that sample. Obviously, the presence of samarium up to a certain concentration stimulated the higher polymerization degree of Ti atoms. The preliminary results exhibited a greater degree of hydrolysis – condensation processes for powders achieved by Ti(IV) butoxide instead of other Ti(IV) alkoxides as a precursor. Our findings correlates well to those made by Xu et al. [42] which found the existence of an optimum doping content of rare earth ion in TiO₂ that improves its properties. The other band at 360 nm could be related to f-f transition of Sm³⁺ ions [43].

CONCLUSIONS

Transparent samarium doped titania gels are prepared from Ti(IV) butoxide with addition of isopropanol in presence only of air moisture. The mixed organic–inorganic amorphous structure is preserved in the samples up to 300 °C. In all compositions TiO₂ (anatase) appeared at 400 °C and its average crystallite size is about 30 nm. By DTA was revealed that at presence of samarium the combus-

tion of organics occurred at higher temperatures (about 340 °C) as compared to pure Ti(IV) butoxide gel (~ 260 °C). The UV-Vis results showed that Sm modified TiO₂ gels exhibited a red shifting of the cut-off in comparison to the pure Ti(IV) butoxide gel. The higher polymerization degree of Ti atoms is achieved for a doping with 1% samarium. The performed analyses (XRD, DTA, IR and UV-Vis) and obtained results allow us to suppose that the sol-gel derived Sm doped TiO₂ thin films will possess similar structural, thermal and optical behavior with the synthesized powders. Additionally, the accumulated knowledge on the characterization of the powders will help us for better understanding the peculiarities of the thin films properties.

Acknowledgements: *The authors are grateful to the financial support of Bulgarian National Science Fund at the Ministry of Education and Science, Contract No DN07/2 14.12.2016.*

REFERENCES

- O. Carp, C. Z. Huisman, A. Reller, *Progress in solid state chemistry*, **32**, 33 (2004).
- S. Sakka, Processing, characterization and applications, vol. I, ed. H. Kozuka, Kluwer Acad. Publishers, 2005, Boston-Dordrecht-London;
- A. Fujishima, T. Rao, D. Tryk, *J. Photochem. Photobiol. C: Photochem. Rev.*, **1**, 1 (2000)
- A. Zaleska, *Recent Patents on Engineering*, **2**, 157 (2008).
- M. Malekshahi Byranvand, A. Nemati Kharat, L. Fathollahi, Z. Malekshahi Beiranvan, *J. Nanostructures*, **3**, 1 (2013).
- L. Wei, Y. Yang, X. Xia, R. Fan, T. Su, et al., *RSC Adv.*, **86**, 1 (2015).
- A. Bokare, M. Pai, A. A. Athawale, *Sol. Energy*, **91**, 111 (2013).
- J. M. Du, H. J. Chen, H. Yang, R. R. Sang, Y. T. Qian, Y. X. Li, G. G. Zhu, Y. J. Mao, W. He and D. J. Kang, *Micropor. Mesopor. Mat.*, **182**, 87-94 (2013).
- C. Leostean, M. Stefan, O. Pana, A. I. Cadis, R. C. Suci, T. D. Silipas and E. Gautron, *J. Alloy Compd.*, **575**, 29-39 (2013).

10. S. Sadhuab and P. Poddar, *RSC Adv.*, **3**, 10363 (2013).
11. J. Reszczyńska, T. Grzyb, J. W. Sobczak, W. Lisowski, M. Gazda, B. Ohtani and A. Zaleska, *Appl. Catal. B-Environ.*, **163**, 40 (2015).
12. D. J. Park, T. Sekino, S. Tsukuda, A. Hayashi, T. Kusunose and S. I. Tanaka, *J. Solid State Chem.*, **184**, 2695 (2011).
13. S. Ezhil Arasi, J. Madhavan and M. Victor Antony Raj, *J. Taibah University for Science*, **12** (2) 186 (2018).
14. E. Madhukar, E. Athare Anil, H. Kolhe Nitin, *Oriental J. Chem.*, **32** (2), 933 (2016).
15. V. Kiisk, M. Šavel, V. Reedo, A. Lukner, I. Sildos, *Phys. Procedia*, **2**, 527 (2009).
16. V. Kiisk, V. Reedo, O. Sild, I. Sildos, *Optical Materials*, **31**, 1376 (2009).
17. A. Stoyanova, N. Ivanova, A. Bachvarova-Nedelcheva, R. Iordanova, *Bulg. Chem. Commun.*, **47** (1), 330 (2015).
18. A. Stoyanova, Ts. Krumova, A. Bachvarova-Nedelcheva, R. Iordanova, *Bulg. Chem. Commun.*, **47**, Special issue C, 118 (2015).
19. A. Bachvarova-Nedelcheva, R. Iordanova, A. Stoyanova, R. Gegova, Y. Dimitriev, A. Loukanov, *Centr. Eur. J. Chem.*, **11** (3), 364 (2013).
20. A. Stoyanova, H. Hitkova, N. Ivanova, A. Bachvarova-Nedelcheva, R. Iordanova, M. Sredkova, *Bulg. Chem. Commun.*, **45** (4), 497 (2013).
21. A. Stoyanova, N. Ivanova, R. Iordanova, A. Bachvarova-Nedelcheva, *Nanoscience and Nanotechnology*, **13**, 166 (2013).
22. S. Jordanov, L. Lakov, I. Stambolova, V. Blaskov, S. Vassilev, V. Dyakova, A. Eliyas, *Compt. Rend. de l'Acad. Bulg. Sci.*, **71**, 625 (2018).
23. S. Jordanov, I. Stambolova, L. Lakov, B. Jivov, V. Blaskov, S. Vasilev, *J. Chem. Technol. Metall.*, **53**, 1179 (2018).
24. J. Dharma, A. Pisal, Simple method of measuring the band gap energy value of TiO₂ in the powder form using a UV/Vis/NIR spectrometer. *Application note*. PerkinElmer, Shelton, CT, (2009).
25. V. Aware Dinkar, S. Jadhav Shridhar, E. Navgire Madhukar, E. Athare Anil and H. Kolhe Nitin, *Orient. J. Chem.*, **32** (2), 933 (2016).
26. G. V. Khade, M. B. Suwarnkar, N. L. Gavade, K. M. Garadkar, *J. Mater Sci: Mater Electron*, **27** (6), 6425 (2016).
27. Wei Niu, Xiaoguo Bi, Gang Wang, Xudong Sun, *Int. J. Electrochem. Sci.*, **8**, 11943 (2013).
28. M. J. Velasco, F. Rubio, J. Rubio, J. Oteo, *Spectr. Lett.*, **32**, 289 (1999).
29. R. Iordanova, A. Bachvarova-Nedelcheva, R. Gegova, Y. Dimitriev, *J. Sol-Gel Sci. Technol.*, **79** (1), 12 (2016).
30. R. Iordanova, R. Gegova, A. Bachvarova-Nedelcheva, Y. Dimitriev, *Phys. Chem. Glasses: Eur. J. Glass Sci. Technol. B*, **56** (4), 128 (2015).
31. St. I. Jordanov, A. D. Bachvarova-Nedelcheva, R. S. Iordanova, *Bulg. Chem. Commun.*, **49** (special issue D), 265 (2017).
32. S. Doeuff, M. Henry, C. Sanchez, J. Livage, *J. Non-Cryst. Sol.*, **89**, 206 (1987).
33. M. Henry, J. Leavage, C. Sanchez, *Progr. Sol. State Chem.*, **18**, 259 (1988).
34. P. D. Moran, G. A. Bowmaker, R. P. Cooney, *Inorg. Chem.*, **37**, 2741 (1998).
35. S. Barboux-Doeuff, C. Sanchez, *Mater. Res. Bull.*, **29**, 1 (1994).
36. X. Gao, IE Wachs, *Cat Today, Catal. Today*, **51**, 233 (1999).
37. V. Barlier, V. Bounor-Legare, G. Boiteux, J. Davenas, *Appl. Surf. Sci.*, **254**, 5408 (2008).
38. A. Bachvarova-Nedelcheva, R. Gegova, A. Stoyanova, R. Iordanova, V. E. Copcia, N. Ivanova, I. Sandu, *Bulg. Chem. Commun.*, **46**, 585 (2014).
39. S. P. Tandon, P. C. Mehta, and R. N. Kapoor, *Z. Naturforsch.*, **25b**, 142 (1970).
40. R. Gegova, A. Bachvarova-Nedelcheva, R. Iordanova, Y. Dimitriev, *Bulg. Chem. Commun.*, **47** (1), 378 (2015).
41. R. Gegova, R. Iordanova, A. Bachvarova-Nedelcheva, Y. Dimitriev, *J. Chem. Technol. Metall.*, **50** (4), 449 (2015).
42. A.-W. Xu, Y. Gao, H.-Q. Lin, *J. Catal.*, **207**, 151 (2002).
43. M. M. Antoinette, S. Israel, *Intern. Res. J. Eng. Techn. (IRJET)*, **04** special iss., 276 (2017).